

Decoupling of non-strange, strange and multi-strange particles from the system in Cu-Cu, Au-Au and Pb-Pb collisions at high energies

M. Waqas^{1,*}, G. X. Peng^{1,2,3 †}, Z. Wazir^{4 ‡}

¹ *School of Nuclear Science and Technology, University of Chinese Academy of Sciences, Beijing 100049, China,*

² *Theoretical Physics Center for Science Facilities, Institute of High Energy Physics, Beijing 100049, China,*

³ *Synergetic Innovation Center for Quantum Effects & Application, Hunan Normal University, Changsha 410081, China*

⁴ *Department of Physics, Ghazi University, Dera Ghazi Khan, Pakistan*

Abstract: Transverse momentum spectra of the non-strange, strange and multi-strange particles in central and peripheral Copper-Copper, Gold-Gold and Lead-Lead collisions are analyzed by the blast wave model with Boltzmann Gibbs statistics. The model results are approximately in agreement with the experimental data measured by BRAHMS, STAR, SPS, NA 49 and WA 97 Collaborations in special transverse momentum ranges. Bulk properties in terms of kinetic freeze out temperature, transverse flow velocity and freezeout volume are extracted from the transverse momentum spectra of the particles. Separate freeze out temperatures are observed for the non-strange, strange and multi-strange particles which maybe due to different reaction cross-sections of the interacting particles and it reveals the triple kinetic freezeout scenario in collisions at BRAHMS, STAR, SPS, NA 49 and WA 97 Collaborations, however the transverse flow velocity and freezeout volume are mass dependent and they decrease with the increasing the rest mass of the particles. Furthermore, the kinetic freezeout temperature, transverse flow velocity and kinetic freezeout volume in central nucleus-nucleus collisions are larger than those in peripheral collisions. Besides, the larger kinetic freezeout temperature and freezeout volume are observed in the most heaviest nuclei collisions, indicating their dependence on the size of interacting system.

Keywords: Decoupling, non-strange, strange, multi-strange, kinetic freeze-out temperature, transverse flow velocity, transverse momentum spectra, high energy collisions.

PACS: 25.75.Ag, 25.75.Dw, 24.10.Pa

1 Introduction

Heavy ion collisions have been used to study the Quark Gluon Plasma (QGP) phase transition into a hadronic gas [1–4] for more than a decade. The phase transition was initially assumed to be either first or second order [5–8], but the quantum chromodynamics (QCD) calculations proved that it is a cross-over [9–11]. There is no single critical temperature in a cross-over phase transition where a phase transition occurs and all the degrees of freedom are going to be switched between the phases. It is impossible to idiomatically define (even though in the case of QCD possibly many exists) the characteristic temperature (T_c) and it depends on what potential order parameter is being observed. Chiral condensate, Polyakov loop and strangeness susceptibility [12] were focused in the early lattice QCD calculations and found a wide range in characteristic tem-

peratures. The most recent lattice QCD calculations has shown an approximate difference of 15-20 MeV in the hadronization temperatures between the light and strange particles [13].

Temperature is one of the most important concept in high energy heavy-ion collisions. Several temperatures namely the initial temperature, chemical freezeout temperature, thermal or kinetic freezeout temperature and the effective temperature are frequently used in the physics of high energy collisions and these temperatures occur at different stages. The initial temperature describes the degree of excitation of an interacting system at the initial stage of collisions. Chemical freeze out is an intermediate stage in high energy collisions where the intra-nuclear collisions among the particles become inelastic and the abundances of stable particles are fixed and the temperature of the particles at the stage is known as the chemical freeze out temperature. Cor-

*Corresponding author. Email (M.Waqas): waqas_phy313@yahoo.com; waqas_phy313@ucas.ac.cn

†Corresponding author. Email (G. X. Peng): gxpeng@ucas.ac.cn

‡author. Email (Z.wazir): zafar_wazir@yahoo.com

respondingly, the thermal freeze out temperature (T_0) describes the excitation degree of interacting system at the last but not the least stage of high energy collisions and the final state particles p_T spectra are determined (frozen) at this stage. Effective temperature is not a real temperature but it describes the sum of excitation degree of interacting system and the effect of transverse flow at the stage of kinetic freeze out. Further details of the temperatures can be found in [14].

T_0 has very complex situation, based on their energy [15–17] and centrality dependence [15–19]. Because of having a complex process, the freezeout shows a hierarchy, where the production of different kinds of particles and reactions cease at different time scales. According to kinetic theory perspective, the reactions with lower interaction cross section decouple early from the system compared to reaction with higher cross section. Besides, the particles decoupling may also depend on its rest mass that reveal the multiple kinetic freeze-out scenario. Furthermore, according to some school of thoughts the single, and double kinetic freezeout scenarios also exists in some literatures, which represents one set of parameters to be used for the spectra of both the strange and non-strange particles in case of single freeze-out scenario, while one set of parameters for strange (or multistrange) particles and another for non-strange (or non-multistrange) particles should be used. In case of multiple kinetic freezeout scenario one should use different sets of parameters for different particles. It is very important to find out the correct kinetic freezeout scenario. In addition, β_T is also an important parameter which reflects the collective expansion of the emission source and it is believed that both T_0 and β_T maybe dependent on the size of interacting nuclei (A-A, p-A and p-p collisions) and heavier interacting systems may give the chance of formation of QGP. The study of various nucleus-nucleus and hadron-nucleus as well as p-p collisions is very useful in understanding the microscopic features of degrees of equilibration and their dependencies on the number of participants in the system. Besides, this study may also provide some useful information about the formation of super hadronic dense matter which is not the focus in this work.

In this paper, our main focal interest is the extraction of kinetic freeze out temperature, transverse flow velocity and freezeout volume from which we can dig out of the correct kinetic freezeout scenario. We will extract the relative parameters from the fitting of transverse momentum (mass) spectra of π^+ , K^+ , p , K_S^0 , Λ , Ξ or $\bar{\Xi}^+$ and $\Omega + \bar{\Omega}$ or $\bar{\Omega}^+$ or $\Omega^- + \Omega^+$ produced in central and peripheral Copper-Copper (Cu-Cu), gold-gold (Au-Au) and lead-lead (Pb-Pb) collisions at 200 GeV, 62.4 GeV and 158 GeV respectively by the blast wave

model with Boltzmann Gibb's statistics. The related parameters are then extracted from the fittings.

The remainder of the paper consists of method and formalism in section 2, followed by the results and discussion in section 3. In section 4, we summarized our main observations and conclusions.

2 The model and method

The spectra of high energy transverse momentum region is generally contributed by the hard scattering process which is described by the Quantum chromodynamics (QCD) calculations [20–23]. The Hagedorn function [23,24], which is an inverse power law, can also be used to describe the hard scattering process. The inverse power law has at least three revisions which can be found in [25–31].

The low transverse momentum region is contributed by the soft excitation process in which the kinetic freeze out temperature and transverse flow velocity can be extracted, however the hard scattering process has no contribution in the extraction of kinetic freeze out temperature and transverse flow velocity. Therefore we will not discuss the hagedorn function and its revisions.

The kinetic freeze out temperature and transverse flow velocity can be extracted by analyzing the spectra in low p_T region by various distributions such as Erlang distribution [32–34], Tsallis distribution [35–37], Tsallis+standard distribution[38–43] and others. We will use the blast wave model with Boltzmann Gibbs statistics [44–46], which is the most direct distribution and having less parameters. Due to the contribution of resonance production in some cases or other reasons such as statistical fluctuation. A single component blast wave model is not enough for the description of spectra in low transverse momentum region, then the two-component blast wave model is required in these special cases.

According to references [44–46], the first component of kinetic freeze out temperature (T_1) and transverse flow velocity (β_{T1}) in the blast wave model with Boltzmann Gibb's (BGBW) statistics results in the probability density function of transverse momentum (p_T) to be

$$f(p_T, T_{01}, \beta_{T1}) = \frac{1}{N} \frac{dN}{dp_T} = C_1 \frac{gV}{(2\pi)^2} p_T m_T \int_0^R r dr \times I_0 \left[\frac{p_T \sinh(\rho_1)}{T_{01}} \right] K_1 \left[\frac{m_T \cosh(\rho_1)}{T_{01}} \right], \quad (1)$$

where C_1 stands for the normalization constant that leads the integral in Eq. (1) to be normalized to 1, N is the number of particles, g is the degeneracy factor

of the particle (which is different for different particles, based on $g_n=2S_n+1$, while S_n is the spin of the particle) $m_T = \sqrt{p_T^2 + m_0^2}$ is the transverse mass, I_0 and K_1 are the modified Bessel functions of the first and second kinds respectively, $\rho = \tanh^{-1}[\beta(r)]$ is the boost angle, $\beta(r) = \beta_S(r/R)^{n_0}$ is a self-similar flow profile and β_S being the flow velocity on the surface, r/R is the relative radial position in the thermal source.

The second component of the blast wave model has the same form as the first one, but with the kinetic freeze out temperature (T_{02}) and transverse flow velocity (β_{T2}). thus, the two component transverse momentum distribution function in blast wave model can be demonstrated as

$$f_0(p_T) = kf(p_T, T_{01}, \beta_{T1}) + (1-k)f(p_T, T_{02}, \beta_{T2}), \quad (2)$$

where k is the contribution fraction of the first component (soft excitation), while $(1-k)$ shows the contribution fraction of the second component (hard scattering) in the Eq. 2. According to Hagedorn thermal model [23], the two-component Boltzmann-Gibbs blast-wave distribution function can also be structured by using the usual step function,

$$f_0(p_T) = \frac{1}{N} \frac{dN}{dp_T} = A_1 \theta(p_1 - p_T) f(p_T, T_{01}, \beta_{T1}) + A_2 \theta(p_T - p_1) f(p_T, T_{02}, \beta_{T2}), \quad (3)$$

where A_1 and A_2 are the fraction constants giving the two components to be equal to each other at $p_T = p_1$, $\theta(p_1 - p_T) = 1$ (or 0), if $p_T < p_1$ (or $p_T > p_1$) and $\theta(p_T - p_1) = 1$ (or 0), if $p_T > p_1$ (or $p_T < p_1$). Both Eq. (2) and (3) can be used for the extraction of T_0 and β_T in the two-component blast wave model i.e

$$T_0 = kT_{01} + (1-k)T_{02}, \quad (4)$$

and

$$\beta_T = k\beta_{T1} + (1-k)\beta_{T2}, \quad (5)$$

If Eq.(2) is used to get the parameter values of the two components, k is directly given by Eq. (2), However, if the parameter of two component values are obtained by using Eq. (3), k is expressed by

$$k = \int_0^{p_1} A_1 f(p_T, T_{01}, \beta_{T1}) dp_T, \quad (6)$$

Because Eq. (3) is the probability density function, it is naturally normalized. The second component in Eq. (2) or (3) is not necessary in the fitting procedure. if the spectra are not in a very wide p_T range, and therefore only the first component in Eq. (2) and Eq.(3), that is,

Eq. (1), can be used to fit the spectra. Although Eq. (2) and Eq.(3) are not used in this work, but they are presented in order to show the complete treatment in methodology.

In some cases, the spectra are not in the form of p_T , but m_T . Then the p_T distribution $f_S(p_T)$ is needed to convert into m_T distribution $f_S(m_T)$ by $f_S(m_T)|dm_T| = f_S(p_T)|dp_T|$ through $p_T|dp_T| = m_T|dm_T|$ due to the invariant cross section. In fact, Eq. (1) appears in the form of $f_S(m_T)$, so we will convert it into $f_S(p_T)$ pragmatically. In the present work, we have analyzed the p_T spectra of the particles (π^+ , K^+ , p , K_S^0 , Λ , Ξ or (Ξ^+) and $\Omega + \bar{\Omega}$ or ($\bar{\Omega}^+$) or ($\Omega^- + \Omega^+$)) by using the single component blast wave model with Boltzman Gibb's statistics and extracted T_0 and β_T . However the spectra in a wide p_T range is not needed for the extraction of T_0 and β_T due to small fraction in high p_T region.

3 Results and discussion

Figures 1-3 demonstrate the p_T or $m_T - m_0$ or m_T spectra, $(1/N_{ev})(1/2\pi m_T)d^2N/dm_T dy$, $(1/2\pi p_T)d^2N/dp_T dy$, $(1/m_T)d^2N/dm_T dy$, $(1/m_T)dN/dm_T$ of π^+ , K^+ , p , K_S^0 , Λ , Ξ or (Ξ^+) and $\Omega + \bar{\Omega}$ or ($\bar{\Omega}^+$ or $\Omega^- + \Omega^+$) produced in central and peripheral Cu-Cu, Au-Au and Pb-Pb collisions at $\sqrt{s_{NN}} = 200$ GeV, 62.4 GeV and 158 GeV respectively, where N denotes the number of particles. The types of particle and collision along with their energies are marked in the panels. The symbols in the figures represent the experimental data measured by BRAHMS [47], STAR [48, 45, 49], SPS [50], NA 49 [51] and WA 97 [52] Collaborations respectively. The curves are our fitted results by using Eq. (1).

The values of the free parameters (T_0 , β_T , V and n), the normalization constant (N_0), χ^2 and the number of degree of freedom (ndof), the concrete collisions, energies, particles, spectra and the amounts scaled for plotting are given in Table 1. The spectra in very low- p_T region are not taken care carefully in the fit process due to the resonance production, while the fit itself is not too good. One can see that the blast-wave fit with Boltzmann Gibb's statistics fit approximately the experimental data over a wide energy range.

The change in trends of the kinetic freeze out temperature (T_0) and transverse flow velocity (β_T) with the rest mass of the particles (m_0) is demonstrated in figure 4. Figure 4(a) shows the dependence of T_0 on m_0 in the central and peripheral Cu-Cu, Au-Au and Pb-Pb collisions at 200 GeV, 62.4 GeV and 158 GeV respectively for the non-strange, strange and multi-strange particles, while the dependence of β_T on m_0 is shown in figure

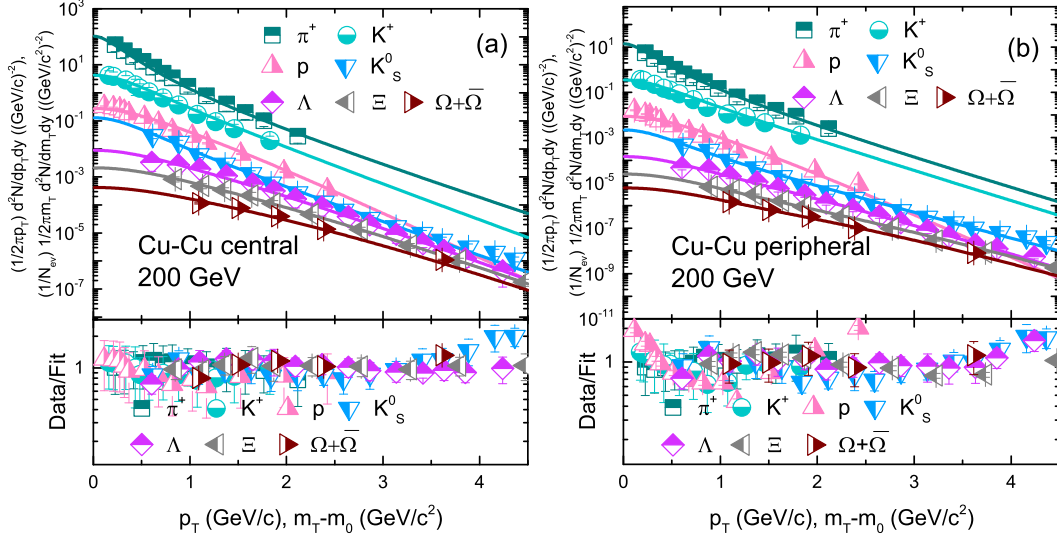


Fig. 1. Transverse momentum spectra of π^+, K^+ and p at rapidity $|y| = 0$ [47], K_S^0 , Λ , Ξ and $\Omega + \bar{\Omega}$ at rapidity $|y| < 0.5$ [48] produced in central (0–10% centrality) and peripheral (50–70% centrality for π^+ , K^+ and p and 40–60% centrality for K_S^0 , Λ , Ξ and $\Omega + \bar{\Omega}$) Cu-Cu collisions at 200 GeV. The symbols represent the experimental data measured by BRAHMS and STAR collaborations [47, 48], while the curves are our fitted results by using the blast wave model with Boltzmann-Gibbs statistics, Eq (1). The corresponding results of data/fit is presented in each panel.

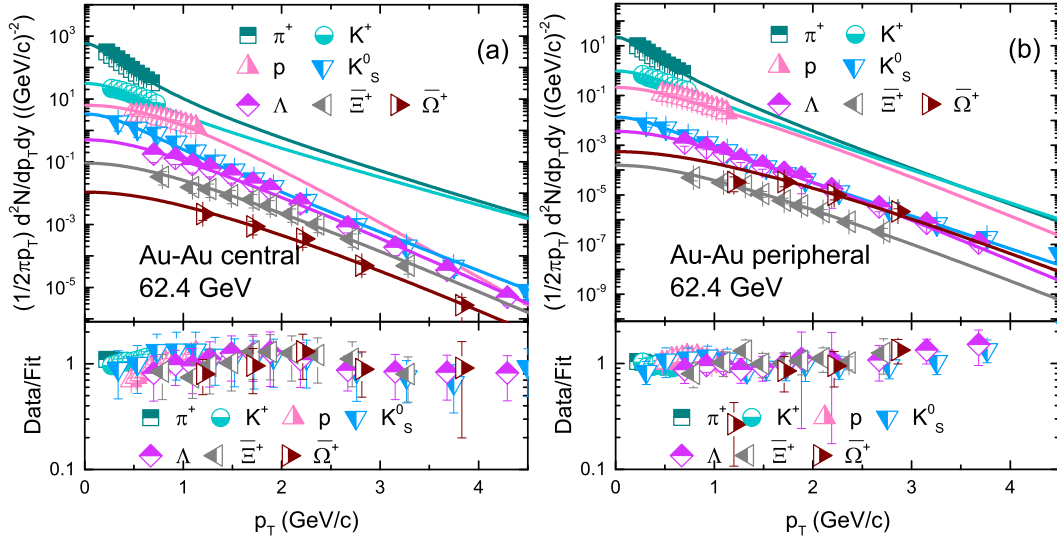


Fig. 2. Transverse momentum spectra of π^+, K^+ and p at mid-rapidity $mid - |y| < 0.1$ [45], K_S^0 , Λ , Ξ^+ and $\bar{\Omega}^+$ at pseudo-rapidity $|\eta| < 1.8$ [49] produced in central (0–5% centrality) and peripheral (70–80% centrality for π^+ , K^+ and p and 60–80% centrality for K_S^0 , Λ , Ξ^+ and $\bar{\Omega}^+$) Au-Au collisions at 62.4 GeV. The symbols represent the experimental data measured by STAR collaboration [45, 49], while the curves are our fitted results by using the blast wave model with Boltzmann-Gibbs statistics, Eq (1). The corresponding results of data/fit is presented in each panel.

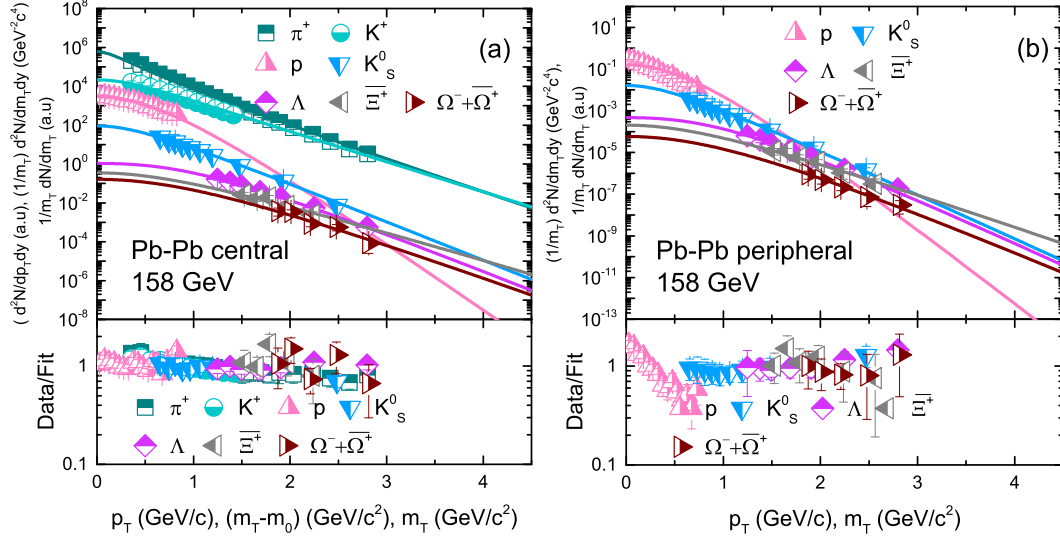


Fig. 3. Transverse momentum spectra of π^+, K^+ [50], p [51] at rapidity interval $2.4 < y < 2.8$ and K_S^0 and Λ at rapidity interval $2 < \eta < 3$, and Ξ^+ and $\Omega^- + \bar{\Omega}^+$ at rapidity interval $3 < \eta < 4$ [52] produced in central and p [51], K_S^0 , Λ , Ξ^+ and $\Omega^- + \bar{\Omega}^+$ [52] in peripheral Pb-Pb collisions at 158 GeV. The symbols represent the experimental data measured by SPS, NA 49 and WA 97 collaborations [50–52], while the curves are our fitted results by using the blast wave model with Boltzmann Gibbs’s statistics, Eq (1). The corresponding results of data/fit is presented in each panel.

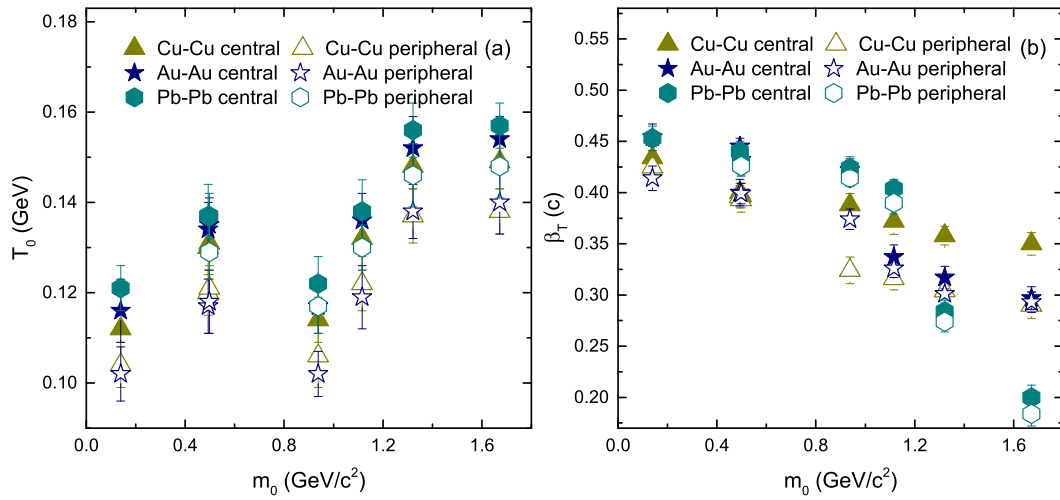


Fig. 4. Dependence of (a) T_0 and (b) β_T on m_0 and centrality.

Table 1. Values of free parameters (T_0 and β_T), normalization constant (N_0), χ^2 , and degree of freedom (dof) corresponding to the curves in Figs. 1–6.

Collisions	Centrality	Particle	Spectrum	scaled by	T_0	β_T	$V(fm^3)$	n_0	N_0
Fig. 1 Cu-Cu 200 GeV	0–10%	π^+	$1/N_{ev}(1/2\pi m_T)d^2N/dm_T dy$	–	0.112 ± 0.008	0.434 ± 0.011	3490 ± 190	1	0.074 ± 0.007
	–	K^+	$1/N_{ev}(1/2\pi m_T)d^2N/dm_T dy$	100	0.130 ± 0.006	0.400 ± 0.009	3000 ± 200	2	$1 \times 10^{-4} \pm 3 \times 10^{-4}$
	–	p	$1/N_{ev}(1/2\pi m_T)d^2N/dm_T dy$	2000	0.114 ± 0.007	0.388 ± 0.012	2730 ± 155	2	$2.7 \times 10^{-7} \pm 4 \times 10^{-7}$
	–	K_S^0	$(1/2\pi p_T)d^2N/dp_T dy$	1/100	0.131 ± 0.005	0.397 ± 0.011	2950 ± 163	2	0.038 ± 0.003
	–	Λ	$(1/2\pi p_T)d^2N/dp_T dy$	1/260	0.132 ± 0.007	0.372 ± 0.013	2500 ± 172	2	0.0047 ± 0.0004
	–	Ξ	$(1/2\pi p_T)d^2N/dp_T dy$	1/100	0.148 ± 0.005	0.358 ± 0.009	2170 ± 186	2	0.0001 ± 0.0000
	–	$\Omega + \bar{\Omega}$	$(1/2\pi p_T)d^2N/dp_T dy$	1/100	0.149 ± 0.006	0.350 ± 0.011	1900 ± 167	2	$1.5 \times 10^{-4} \pm 4 \times 10^{-4}$
	50–70%	π^+	$1/N_{ev}(1/2\pi m_T)d^2N/dm_T dy$	–	0.102 ± 0.005	0.425 ± 0.009	2570 ± 160	2	0.012 ± 0.003
	–	K^+	$1/N_{ev}(1/2\pi m_T)d^2N/dm_T dy$	100	0.120 ± 0.005	0.396 ± 0.011	2300 ± 150	2	$9 \times 10^{-6} \pm 7 \times 10^{-6}$
	–	p	$1/N_{ev}(1/2\pi m_T)d^2N/dm_T dy$	700	0.106 ± 0.005	0.324 ± 0.013	2000 ± 240	2	$2 \times 10^{-8} \pm 4 \times 10^{-8}$
	40–60%	K_S^0	$(1/2\pi p_T)d^2N/dp_T dy$	10	0.121 ± 0.007	0.393 ± 0.012	2226 ± 191	2.3	$6.5 \times 10^{-7} \pm 5 \times 10^{-7}$
	–	Λ	$(1/2\pi p_T)d^2N/dp_T dy$	3	0.122 ± 0.006	0.316 ± 0.011	1800 ± 140	2.8	$1.48 \times 10^{-7} \pm 3 \times 10^{-7}$
	–	Ξ	$(1/2\pi p_T)d^2N/dp_T dy$	7	0.137 ± 0.006	0.304 ± 0.012	1600 ± 153	3	$1.7 \times 10^{-8} \pm 4 \times 10^{-8}$
	–	$\Omega + \bar{\Omega}$	$(1/2\pi p_T)d^2N/dp_T dy$	10	0.138 ± 0.005	0.290 ± 0.013	1400 ± 150	3	$2.12 \times 10^{-7} \pm 2 \times 10^{-7}$
Fig. 2 Au-Au 62.4 GeV	0–5%	π^+	$(1/2\pi p_T)d^2N/dp_T dy$	–	0.116 ± 0.007	0.454 ± 0.013	5900 ± 220	2	0.3 ± 0.004
	–	K^+	$(1/2\pi p_T)d^2N/dp_T dy$	–	0.134 ± 0.006	0.445 ± 0.008	5500 ± 190	2	0.05 ± 0.006
	–	p	$(1/2\pi p_T)d^2N/dp_T dy$	0.5	0.117 ± 0.006	0.422 ± 0.011	5000 ± 212	1	0.025 ± 0.005
	–	K_S^0	$(1/2\pi p_T)d^2N/dp_T dy$	1/8	0.135 ± 0.006	0.432 ± 0.013	5487 ± 200	2	0.006 ± 0.0005
	–	Λ	$(1/2\pi p_T)d^2N/dp_T dy$	1/7	0.136 ± 0.006	0.337 ± 0.012	4700 ± 200	3	0.0045 ± 0.0003
	–	Ξ^+	$(1/2\pi p_T)d^2N/dp_T dy$	1/5	0.152 ± 0.007	0.317 ± 0.011	4321 ± 213	2	$8 \times 10^{-4} \pm 4 \times 10^{-4}$
	–	$\bar{\Omega}^+$	$(1/2\pi p_T)d^2N/dp_T dy$	1/5	0.154 ± 0.005	0.297 ± 0.011	4000 ± 189	2	0.032 ± 0.005
	70–80%	π^+	$(1/2\pi p_T)d^2N/dp_T dy$	–	0.102 ± 0.006	0.414 ± 0.012	5200 ± 198	2	0.008 ± 0.0003
	–	K^+	$(1/2\pi p_T)d^2N/dp_T dy$	–	0.117 ± 0.006	0.400 ± 0.013	5000 ± 221	2	0.0012 ± 0.0001
	–	p	$(1/2\pi p_T)d^2N/dp_T dy$	1/2	0.102 ± 0.007	0.374 ± 0.010	4700 ± 180	2	$5 \times 10^{-4} \pm 4 \times 10^{-4}$
	60–80%	K_S^0	$(1/2\pi p_T)d^2N/dp_T dy$	10^4	0.118 ± 0.005	0.399 ± 0.010	4950 ± 168	2	$1.6 \times 10^{-9} \pm 3 \times 10^{-9}$
	–	Λ	$(1/2\pi p_T)d^2N/dp_T dy$	10^4	0.119 ± 0.007	0.327 ± 0.09	4340 ± 165	2	$5 \times 10^{-10} \pm 6 \times 10^{-10}$
	–	Ξ^+	$(1/2\pi p_T)d^2N/dp_T dy$	10^3	0.138 ± 0.006	0.301 ± 0.012	4000 ± 186	2	$3 \times 10^{-10} \pm 6 \times 10^{-10}$
	–	$\bar{\Omega}^+$	$(1/2\pi p_T)d^2N/dp_T dy$	80	0.140 ± 0.007	0.293 ± 0.010	3725 ± 152	2	$9 \times 10^{-9} \pm 4 \times 10^{-9}$
	Central	π^+	$(1/2\pi p_T)d^2N/dp_T dy$	–	0.121 ± 0.005	0.453 ± 0.012	7300 ± 300	1	169.17 ± 32
	–	K^+	$(1/2\pi p_T)d^2N/dp_T dy$	–	0.137 ± 0.007	0.435 ± 0.010	7000 ± 220	1	23.17 ± 6
	0–5%	p	$(1/m_T)d^2N/dm_T dy$	60	0.122 ± 0.005	0.424 ± 0.011	6670 ± 190	–2	0.02 ± 0.004
	Central	K_S^0	$(1/m_T)dN/dm_T$	50	0.137 ± 0.006	0.430 ± 0.013	6960 ± 196	0	0.0017 ± 0.0001
Fig. 3 Pb-Pb 158 GeV	–	Λ	$(1/m_T)dN/dm_T$	–	0.138 ± 0.007	0.404 ± 0.009	6400 ± 185	0	0.0016 ± 0.0001
	–	Ξ^+	$(1/m_T)dN/dm_T$	1/27	0.156 ± 0.006	0.284 ± 0.011	6113 ± 183	2	0.014 ± 0.004
	–	$\Omega^- + \bar{\Omega}^+$	$(1/m_T)dN/dm_T$	1/180	0.157 ± 0.005	0.200 ± 0.012	5800 ± 200	2	0.022 ± 0.003
	43–100%	p	$(1/m_T)d^2N/dm_T dy$	1/10	0.117 ± 0.006	0.414 ± 0.008	6000 ± 210	–2	$6 \times 10^{-5} \pm 3 \times 10^{-5}$
	Peripheral	K_S^0	$(1/m_T)dN/dm_T$	20	0.129 ± 0.006	0.426 ± 0.010	6280 ± 200	0	$7 \times 10^{-7} \pm 5 \times 10^{-7}$
	–	Λ	$(1/m_T)dN/dm_T$	–	0.130 ± 0.005	0.390 ± 0.011	5700 ± 215	0	$7 \times 10^{-7} \pm 3 \times 10^{-7}$
	–	Ξ^+	$(1/m_T)dN/dm_T$	1/20	0.146 ± 0.007	0.274 ± 0.010	5413 ± 180	2	$5 \times 10^{-6} \pm 4 \times 10^{-6}$
	–	$\Omega^- + \bar{\Omega}^+$	$(1/m_T)dN/dm_T$	1/300	0.148 ± 0.007	0.184 ± 0.012	5000 ± 210	2	$4 \times 10^{-6} \pm 3 \times 10^{-6}$

4(b). Different collisions are represented by different symbols. The solid and open symbols represent the central and peripheral collisions respectively.

At present, one can see that T_0 has no clear dependence on m_0 . π^+ and p has lower value for T_0 than all of the strange and multi-strange particles and they decouple from the system at the same time. K^+ and K_S^0 are lighter than proton but they both decouple early from the system and freeze out earlier than proton. This result is inconsistent with [16, 35, 53] (which shows the obvious mass dependence of T_0), but is consistent with [54], although the main idea in [54] is different from our current work but larger T_0 for K^+ and K_S^0 than proton can be seen.

In the present work, It is observed that the K-F-O temperature of the multi-strange particles is considerably larger than those of the strange particles and the later is larger than the non-strange particles, which reveal a picture of separate freeze out processes for the non-strange, strange and multi-strange particles. We believe that the reason behind the very large kinetic freeze out temperature of multi-strange particles followed by strange particles maybe the interaction cross-section, such that if the multi-strange (strange particles) hadrons don't interact with other hadrons, their cross-section is small and hence they decouple early from the system, which allow their early freeze out.

Further more the kinetic freeze out temperature in Cu-Cu, Au-Au and Pb-Pb central collisions is larger than in peripheral collisions, and T_0 for all the particles in Cu-Cu central and peripheral collisions is smaller than in Au-Au central and peripheral collisions and the later is smaller than in Pb-Pb central and peripheral collisions, which exhibits the dependence of T_0 on size of interacting system. The larger T_0 in the most heaviest nuclei and central collisions is due to the fact that more number of nucleons are involved in the heavy nuclei and in most central interactions which lead the system to higher excitation degree but a variety of data maybe needed (hadron-hadron, hadron-nucleus, different nucleus-nucleus collisions) to further analyze this work in the future.

Figure 4(b) shows the variation of β_T with m_0 . One can see that β_T is slightly larger in central collisions than in the peripheral collisions. Furthermore, it is observed that β_T decrease with increasing mass of the particle which indicates the early decoupling of heavier particles from the system that results in their early freeze out of heavy particles. This result is consistent with [16, 18, 55]. No dependence of β_T on energy or size of the interacting system is observed in this work.

Figure 5 is the same as Fig4. but it demonstrates the variation of V with m_0 and centrality for the non-

strange, strange and multi-strange particles in Cu-Cu, Au-Au and Pb-Pb central and peripheral collisions at 200, 62.4 and 158 GeV respectively. Different symbols are used to represent different particles, while the solid and open symbols represent the central and peripheral collisions respectively. One can see the larger V for light particles which decrease for heavier particles that leads to the volume differential freezeout scenario. Compared to the peripheral collisions, the central collisions correspond to larger larger V due large number of participant nucleons which indicates the quick approach of the later system to equilibrium state. Furthermore, V is observed to be dependant on the size of the interacting system as it is larger in Pb-Pb collisions than in Au-Au collisions, and in later it is larger than in Cu-Cu collisions.

Figure 6 (a)-(c) shows the co-relation of T_0 and V . The solid and open symbols are used for the central and peripheral collisions respectively and different particles are represented by different symbols. T_0 decrease with the increase of V in the most central and most peripheral heavy ion (Cu-Cu, Au-Au and Pb-Pb) collisions.

Figure 7 is the same to Fig 4. but it demonstrates the dependence of N_0 with m_0 and centrality. N_0 is not just a normalization constant but it reflects the multiplicity. One can see larger N_0 in central collisions compared to the peripheral collisions. At present, there is no dependence of N_0 on m_0 .

4 Conclusions

We summarize here our main observations and conclusions.

(a) The transverse momentum spectra of non-strange, strange and multi-strange particles produced in central and peripheral Cu-Cu, Au-Au and Pb-Pb collisions have been analyzed by BGBW model. The model results are in agreement with the experimental data in the special p_T range measured by BRAHMS, STAR, SPS, NA 49 and WA 97 collaborations.

(b) Separate kinetic freezeout scenario for non-strange, strange and multi-strange particles are found which shows the dependence of the kinetic freezeout temperature of the particles on their interaction cross-section and reveals the triple kinetic freeze out scenario, However β_T and V are mass dependent which decrease with increasing m_0 .

(c) Kinetic freeze out temperature (T_0), transverse flow velocity (β_T) and kinetic freezeout volume (V) are extracted from the transverse momentum spectra fitting to the experimental data. It is observed that T_0 , β_T and V are slightly larger in central collisions than in the peripheral collisions, and T_0 and V is also generally larger

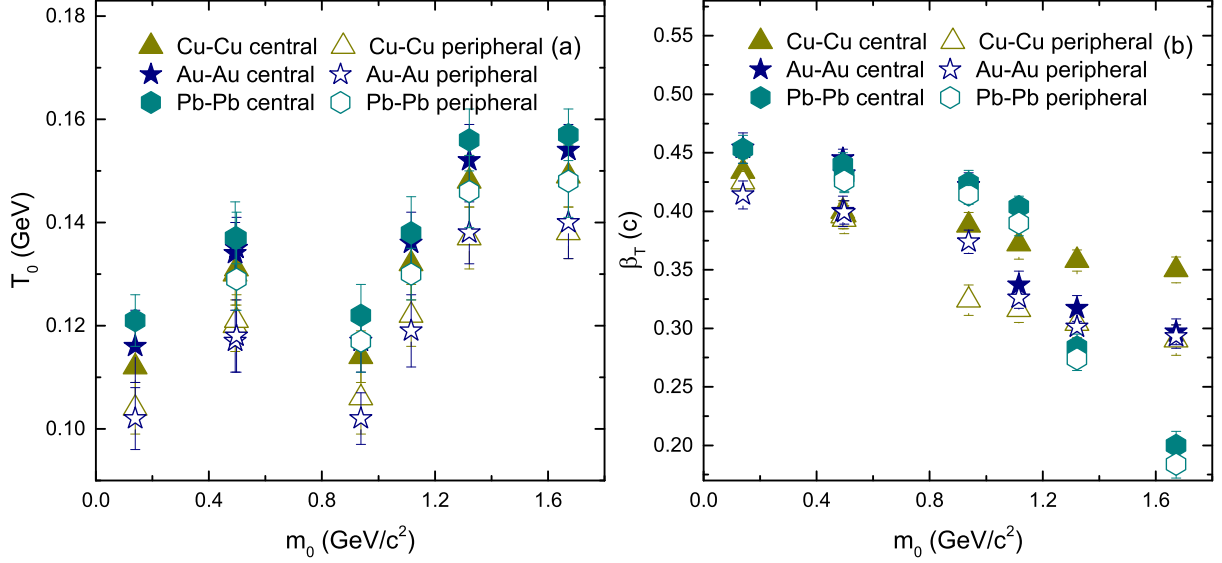


Fig. 5. Variation of V with m_0 and centrality for non-strange, strange and multi-strange particles in Cu-Cu, Au-Au and Pb-Pb central and peripheral collisions.

in the most heaviest interacting system, while β_T shows no dependence on the size of interacting system.

d) The normalization constant (N_0) that reflects multiplicity, is larger in central collisions than in peripheral collisions.

Data availability

The data used to support the findings of this study are included within the article and are cited at relevant places within the text as references.

Compliance with Ethical Standards

The authors declare that they are in compliance with ethical standards regarding the content of this paper.

Acknowledgements

The authors would like to thank support from the National Natural Science Foundation of China (Grant Nos. 11875052, 11575190, and 11135011).

References

- [1] Arsene, I., *et al.* [BRAHMS], “Quark gluon plasma and color glass condensate at RHIC? The Perspective from the BRAHMS experiment,” Nucl. Phys. A **757**, 1 (2005).
- [2] Adcox, K., *et al.* [PHENIX], “Formation of dense partonic matter in relativistic nucleus-nucleus collisions at RHIC: Experimental evaluation by the PHENIX collaboration,” Nucl. Phys. A **757**, 184 (2005). doi:10.1016/j.nuclphysa.2005.03.086
- [3] Adams, J., *et al.* [STAR], “Experimental and theoretical challenges in the search for the quark gluon plasma: The STAR Collaboration’s critical assessment of the evidence from RHIC collisions,” Nucl. Phys. A **757**, 102 (2005). doi:10.1016/j.nuclphysa.2005.03.085 [arXiv:nucl-ex/0501009 [nucl-ex]]
- [4] Back, B. B., *et al.* [PHOBOS], “The PHOBOS perspective on discoveries at RHIC,” Nucl. Phys. A **757**, 28 (2005). doi:10.1016/j.nuclphysa.2005.03.084 [arXiv:nucl-ex/0410022 [nucl-ex]].
- [5] McLerran, L. D and Svetitsky, B., “Quark Liberation at High Temperature: A Monte Carlo Study of SU(2) Gauge Theory,” Phys. Rev. D **24**, 450 (1981). doi:10.1103/PhysRevD.24.450
- [6] Huovinen, P., Kolb, P. F., Heinz, U. W., Ruuskanen, P. V and Voloshin, S. A., “Radial and elliptic flow at RHIC: Further predictions,” Phys. Lett. B **503**, 58-64 (2001). doi:10.1016/S0370-2693(01)00219-2 [arXiv:hep-ph/0101136 [hep-ph]].
- [7] Engels, J., Karsch, F., Satz, H and Montvay, I., “High Temperature SU(2) Gluon Matter on the Lattice,” doi:10.1016/0370-2693(81)90497-4
- [8] Boyd, G. *et al.* “Thermodynamics of SU(3) lattice gauge theory,” Nucl. Phys. B **469**, 419-444 (1996). doi:10.1016/0550-3213(96)00170-8 [arXiv:hep-lat/9602007 [hep-lat]].
- [9] Borsanyi, S., Endrodi, G., Fodor, Z., Jakovac, A., Katz, S. D., Krieg, S., Ratti, C and Szabo, K. K., “The QCD equation of state with dynamical quarks,” JHEP **11**, 077 (2010). doi:10.1007/JHEP11(2010)077 [arXiv:1007.2580 [hep-lat]].
- [10] Borsanyi, S., *et al.* [Wuppertal-Budapest], “Is there still any T_c mystery in lattice QCD? Results with physical masses in the continuum limit III,”

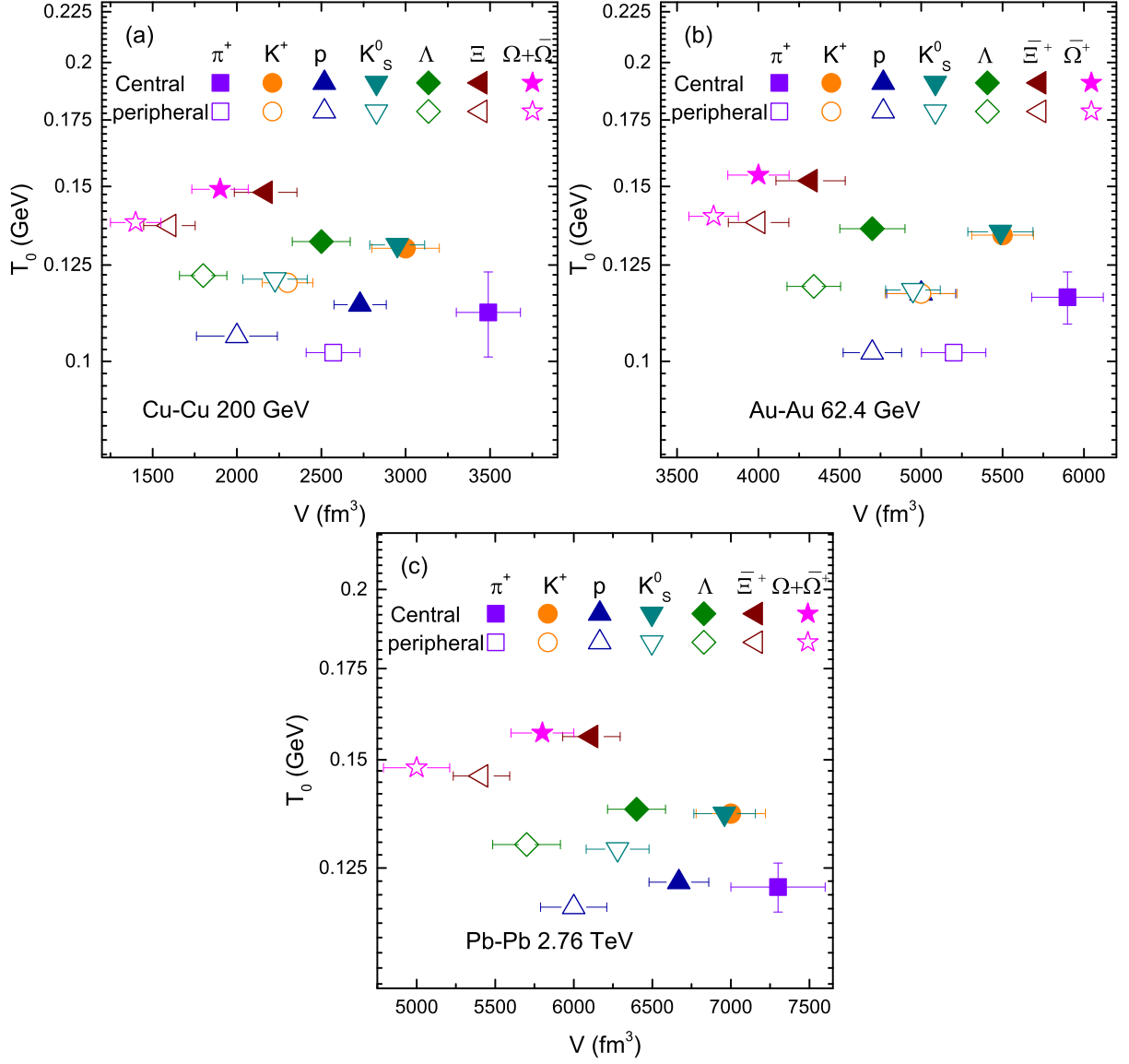


Fig. 6. Variation of T_0 with V for non-strange, strange and multi-strange particles in Cu-Cu, Au-Au and Pb-Pb central and peripheral collisions.

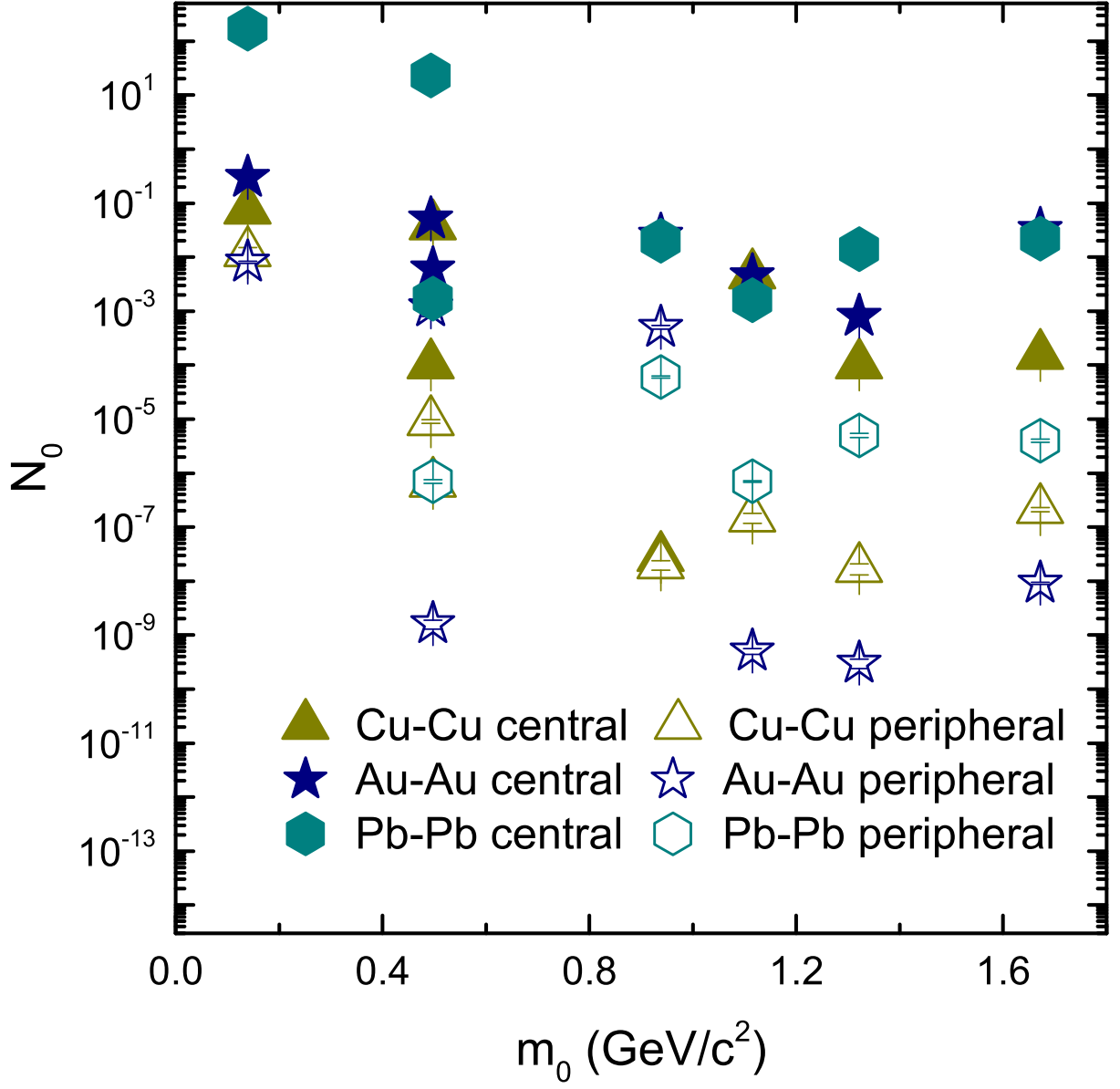


Fig. 7. Variation of N_0 with m_0 and centrality for non-strange, strange and multi-strange particles in Cu-Cu, Au-Au and Pb-Pb central and peripheral collisions.

- JHEP **09**, 073 (2010). doi:10.1007/JHEP09(2010)073 [arXiv:1005.3508 [hep-lat]].
- [11] Aoki, Y., Endrodi, G., Fodor, Z., Katz, S. D., and Szabo, K. K., “The Order of the quantum chromodynamics transition predicted by the standard model of particle physics,” *Nature* **443**, 675-678 (2006). doi:10.1038/nature05120 [arXiv:hep-lat/0611014 [hep-lat]].
- [12] Aoki, Y., Fodor, Z., Katz, S. D. and Szabo, K. K., “The QCD transition temperature: Results with physical masses in the continuum limit,” *Phys. Lett. B* **643**, 46-54 (2006). doi:10.1016/j.physletb.2006.10.021 [arXiv:hep-lat/0609068 [hep-lat]].
- [13] Bellwied, R., Borsanyi, R., Fodor, Z., Katz, S. D. and Ratti, C., “Is there a flavor hierarchy in the deconfinement transition of QCD?,” *Phys. Rev. Lett.* **111**, 202302 (2013). doi:10.1103/PhysRevLett.111.202302 [arXiv:1305.6297 [hep-lat]].
- [14] M. Waqas and F. H. Liu, “Initial, effective, and kinetic freeze-out temperatures from transverse momentum spectra in high-energy proton(deuteron)–nucleus and nucleus–nucleus collisions,” *Eur. Phys. J. Plus* **135**, no.2, 147 (2020) doi:10.1140/epjp/s13360-020-00213-1 [arXiv:1911.01709 [hep-ph]].
- [15] Adamczyk, L. *et al.* [STAR], “Bulk Properties of the Medium Produced in Relativistic Heavy-Ion Collisions from the Beam Energy Scan Program,” *Phys. Rev. C* **96**, 044904 (2017). doi:10.1103/PhysRevC.96.044904 [arXiv:1701.07065 [nucl-ex]].
- [16] Waqas, M., Liu, F. H., Wang, R. Q. and Siddique, I., “Energy scan/dependence of kinetic freeze-out scenarios of multi-strange and other identified particles in central nucleus-nucleus collisions,” *Eur. Phys. J. A* **56**, 188 (2020). doi:10.1140/epja/s10050-020-00192-y [arXiv:2007.00825 [hep-ph]].
- [17] Kumar, L, et al. (STAR Collaboration), “Systematics of kinetic freeze-out properties in high energy collisions from STAR,” *Nucl. Phys. A* **931**, 1114 (2014).
- [18] Lao, H. L., Liu, F. H., Li, B. C. and Duan, M. Y., “Kinetic freeze-out temperatures in central and peripheral collisions: Which one is larger?,” *Nucl. Sci. Tech.* **29**, 82 (2018). doi:10.1007/s41365-018-0425-x [arXiv:1703.04944 [nucl-th]].
- [19] Waqas, M. and Li, B. L., “Kinetic freeze-out temperature and transverse flow velocity in Au-Au collisions at RHIC-BES energies,” *High Energy Phys* 2020, 1787183 (2020).
- [20] Odorico, R., “DOES A TRANSVERSE ENERGY TRIGGER ACTUALLY TRIGGER ON LARGE P(T) JETS?,” *Phys. Lett. B* **118**, 151 (1982).
- [21] Arnison, G. *et al.* [UA1], “Transverse Momentum Spectra for Charged Particles at the CERN Proton anti-Proton Collider,” *Phys. Lett. B* **118**, 167-172 (1982). doi:10.1016/0370-2693(82)90623-2
- [22] M. Biyajima, T. Mizoguchi and N. Suzuki, “Analyses of whole transverse momentum distributions in $p\bar{p}$ and pp collisions by using a modified version of Hagedorn’s formula,” *Int. J. Mod. Phys. A* **32**, no.11, 1750057 (2017) doi:10.1142/S0217751X17500579 [arXiv:1604.01264 [hep-ph]].
- [23] Hagedorn, R., “Multiplicities, p_T distributions and the expected hadron \rightarrow quark-gluon phase tranistion,” *Riv. Nuovo Cimento*, **6**(10), 1 (1983), https://doi.org/10.1007/BF02740917.
- [24] Abelev, B. B. *et al.* [ALICE], “Production of $\Sigma(1385)^\pm$ and $\Xi(1530)^0$ in proton-proton collisions at $\sqrt{s} = 7$ TeV,” *Eur. Phys. J. C* **75**, 1 (2015). doi:10.1140/epjc/s10052-014-3191-x [arXiv:1406.3206 [nucl-ex]].
- [25] Aamodt, K. *et al.* [ALICE], “Transverse momentum spectra of charged particles in proton-proton collisions at $\sqrt{s} = 900$ GeV with ALICE at the LHC,” *Phys. Lett. B* **693**, 53-68 (2010). doi:10.1016/j.physletb.2010.08.026 [arXiv:1007.0719 [hep-ex]].
- [26] Abt, I. *et al.* [HERA-B], “ K^0 and ϕ meson production in proton-nucleus interactions at $s^{1/2} = 41.6$ -GeV,” *Eur. Phys. J. C* **50**, 315-328 (2007). doi:10.1140/epjc/s10052-007-0237-3 [arXiv:hep-ex/0606049 [hep-ex]].
- [27] Abelev, B. *et al.* [ALICE], “Light vector meson production in pp collisions at $\sqrt{s} = 7$ TeV,” *Phys. Lett. B* **710**, 557-568 (2012). doi:10.1016/j.physletb.2012.03.038 [arXiv:1112.2222 [nucl-ex]].
- [28] De Falco, A. [ALICE], “Vector meson production in pp collisions at $\sqrt{s} = 7$ TeV, measured with the ALICE detector,” *J. Phys. G* **38**, 124083 (2011). doi:10.1088/0954-3899/38/12/124083 [arXiv:1106.4140 [nucl-ex]].
- [29] Abelev, B. *et al.* [ALICE], “Inclusive J/ψ production in pp collisions at $\sqrt{s} = 2.76$ TeV,” *Phys. Lett. B* **718**, 295-306 (2012). doi:10.1016/j.physletb.2012.10.078 [arXiv:1203.3641 [hep-ex]].
- [30] Lakomov, I. [ALICE], “Event activity dependence of inclusive J/ψ production in p-Pb collisions at $\sqrt{s_{NN}} = 5.02$ TeV with ALICE at the LHC,” *Nucl. Phys. A* **931**, 1179-1183 (2014). doi:10.1016/j.nuclphysa.2014.08.062 [arXiv:1408.0702 [hep-ex]].
- [31] B. Abelev *et al.* [ALICE], “Heavy flavour decay muon production at forward rapidity in proton–proton collisions at $\sqrt{s} = 7$ TeV,” *Phys. Lett. B* **708**, 265-275 (2012) doi:10.1016/j.physletb.2012.01.063 [arXiv:1201.3791 [hep-ex]].
- [32] Liu, F. H., Gao, Y. Q., Tian, T. and Li, B. C., “Unified description of transverse momentum spectrums contributed by soft and hard processes in high-energy nuclear collisions,” *Eur. Phys. J. A* **50**, 94 (2014). doi:10.1140/epja/i2014-14094-9
- [33] Gao, L. N., Liu, F. H. and Lacey, R. A., “Excitation functions of parameters in Erlang distribution, Schwinger mechanism, and Tsallis statistics in RHIC BES program,” *Eur. Phys. J. A* **52**, 137 (2016). doi:10.1140/epja/i2016-16137-7 [arXiv:1604.07218 [hep-ph]].

- [34] Xie. W. J, “Transverse momentum spectra in high-energy nucleus-nucleus, proton-nucleus and proton-proton collisions,” *Chin. Phys. C* **35**, 1111-1119 (2011). doi:10.1088/1674-1137/35/12/006
- [35] Lao. H. L, Wei. H. R, Liu. F. H and Lacey. R. A, “An evidence of mass-dependent differential kinetic freeze-out scenario observed in Pb-Pb collisions at 2.76 TeV,” *Eur. Phys. J. A* **52**, 203 (2016). doi:10.1140/epja/i2016-16203-2 [arXiv:1601.00045 [nucl-th]].
- [36] Jiang. K, Zhu *et al.* “Onset of radial flow in p+p collisions,” *Phys. Rev. C* **91**, 024910 (2015). doi:10.1103/PhysRevC.91.024910
- [37] Cleymans. J and Worku. D, “Relativistic Thermodynamics: Transverse Momentum Distributions in High-Energy Physics,” *Eur. Phys. J. A* **48**, 160 (2012).
- [38] Barnafoldi. G. G, Urmossy. K and Biro. T. S, “Tsallis-Pareto like distributions in hadron-hadron collisions,” *J. Phys. Conf. Ser.* **270**, 012008 (2011). doi:10.1088/1742-6596/270/1/012008
- [39] Parvan. A. S and Bhattacharyya. T, “Remarks on the phenomenological Tsallis distributions and their link with the Tsallis statistics,” [arXiv:1904.02947 [cond-mat.stat-mech]].
- [40] Conroy. J. M and Miller. H. G, “Color Superconductivity and Tsallis Statistics,” *Phys. Rev. D* **78**, 054010 (2008). doi:10.1103/PhysRevD.78.054010 [arXiv:0801.0360 [hep-ph]].
- [41] Biro. G., Barnafoldi. G. G, Biro. T. S and Urmossy. K, “Application of the Non-extensive Statistical Approach to High Energy Particle Collisions,” *AIP Conf. Proc.* **1853**, 080001 (2017). doi:10.1063/1.4985366 [arXiv:1608.01643 [hep-ph]].
- [42] Teweldeberhan. A. M., Plastino. A. R., and Miller. H. G., “On the cut-off prescriptions with power-law generalized thermostatics,” *Phys. Lett. A* **343**, 71 (2004). doi:10.1016/j.physleta.2005.06.026
- [43] Conroy. J. M., Miller. H. G., and Plastino. A. R., “Thermodynamic Consistency of the q -Deformed Fermi-Dirac Distribution in Nonextensive Thermostatics,” *Phys. Lett. A* **374**, 4581-4584, (2010). doi:10.1016/j.physleta.2010.09.038
- [44] Schnedermann. E, Sollfrank. J and Heinz. U. W, “Thermal phenomenology of hadrons from 200-A/GeV S+S collisions,” *Phys. Rev. C* **48**, 2462-2475 (1993). doi:10.1103/PhysRevC.48.2462 [arXiv:nucl-th/9307020 [nucl-th]].
- [45] Abelev. B. I *et al.* [STAR], “Systematic Measurements of Identified Particle Spectra in pp, d^+ Au and Au+Au Collisions from STAR,” *Phys. Rev. C* **79**, 034909 (2009). doi:10.1103/PhysRevC.79.034909 [arXiv:0808.2041 [nucl-ex]].
- Khuntia. A., Sharma. H., Kumar Tiwari. S, Sahoo. R and Cleymans. J, “Radial flow and differential freeze-out in proton-proton collisions at $\sqrt{s} = 7$ TeV at the LHC,” *Eur. Phys. J. A* **55**, 3 (2019). doi:10.1140/epja/i2019-12669-6 [arXiv:1808.02383 [hep-ph]].
- [46] Arsene. I. C *et al.* [BRAHMS], “Rapidity and centrality dependence of particle production for identified hadrons in Cu+Cu collisions at $\sqrt{s_{NN}} = 200$ GeV,” *Phys. Rev. C* **94**, 014907 (2016). doi:10.1103/PhysRevC.94.014907 [arXiv:1602.01183 [nucl-ex]].
- [47] Agakishiev. G *et al.* [STAR], “Strangeness Enhancement in Cu+Cu and Au+Au Collisions at $\sqrt{s_{NN}} = 200$ GeV,” *Phys. Rev. Lett.* **108**, 072301 (2012). doi:10.1103/PhysRevLett.108.072301 [arXiv:1107.2955 [nucl-ex]].
- [48] Aggarwal. M. M *et al.* [STAR], “Strange and Multi-strange Particle Production in Au+Au Collisions at $\sqrt{s_{NN}} = 62.4$ GeV,” *Phys. Rev. C* **83**, 024901 (2011). doi:10.1103/PhysRevC.83.024901 [arXiv:1010.0142 [nucl-ex]].
- [49] Shao. M *et al.* “Examine the species and beam-energy dependence of particle spectra using Tsallis Statistics,” *J. Phys. G* **37**, 085104 (2010). doi:10.1088/0954-3899/37/8/085104 [arXiv:0912.0993 [nucl-ex]].
- [50] Alt. C *et al.* [NA49], “Energy and centrality dependence of anti-p and p production and the anti-Lambda/anti-p ratio in Pb+Pb collisions between 20/A-GeV and 158/A-GeV,” *Phys. Rev. C* **73**, 044910 (2006). doi:10.1103/PhysRevC.73.044910
- [51] Antinori. F *et al.* [WA97], “Transverse mass spectra of strange and multistrange particles in Pb Pb collisions at 158-A-GeV/c,” *Eur. Phys. J. C* **14**, 633-641 (2000). doi:10.1007/s100520000386
- [52] Thakur. D., Tripathy. S., Garg. P, Sahoo. R and Cleymans. J, “Indication of a Differential Freeze-out in Proton-Proton and Heavy-Ion Collisions at RHIC and LHC energies,” *Adv. High Energy Phys.* **2016**, 4149352 (2016). doi:10.1155/2016/4149352 [arXiv:1601.05223 [hep-ph]].
- [53] Bashir. I. U and Uddin. S, “Kinetic Freeze-out Spectra of Identified Particles Produced in p-Pb Collisions at $\sqrt{s_{NN}} = 5.02$ TeV,” *J. Exp. Theor. Phys.* **124**, 429-432 (2017). doi:10.1134/S1063776117030013 [arXiv:1510.08582 [hep-ph]].
- [54] Wang. Q and Liu. F. H, “Initial and final state temperatures of antiproton emission sources in high energy collisions,” *Int. J. Theor. Phys.* **58**, 4119-4138 (2019). doi:10.1007/s10773-019-04278-2 [arXiv:1909.02390 [hep-ph]].

